LA-UR- 09-00847

Approved for public release; distribution is unlimited.

Title:	Gamma and Neutron Detection in the Nuclear Detection Figure of Merit (NDFOM) Portal
Author(s):	Phillip D. Stroud and Kevin J. Saeger
Intended for:	submission to Annals of Operations Research

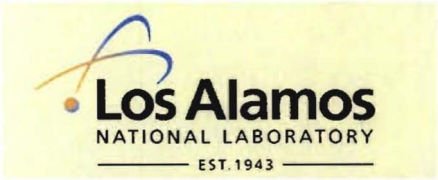

Form 836 (7/06)

Gamma and Neutron Detection Modeling in the Nuclear Detection Figure Of Merit (NDFOM) Portal

Phillip D. Stroud and Kevin J. Saeger
Los Alamos National Laboratory

Abstract

The Nuclear Detection Figure Of Merit (NDFOM) portal is a database of objects and algorithms for evaluating the performance of radiation detectors to detect nuclear material. This paper describes the algorithms used to model the physics and mathematics of radiation detection. As a first-principles end-to-end analysis system, it starts with the representation of the gamma and neutron spectral fluxes, which are computed with the particle and radiation transport code MCNPX. The gamma spectra emitted by uranium, plutonium, and several other materials of interest are described. The impact of shielding and other intervening material is computed by the method of build-up factors. The interaction of radiation with the detector material is computed by a detector response function approach. The construction of detector response function matrices based on MCNPX simulation runs is described in detail. Neutron fluxes are represented in a three-group formulation to treat differences in detector sensitivities to thermal, epithermal, and fast neutrons.

1 Introduction

The nuclear detection figure-of-merit (NDFOM) server[1] provides a database of commercially available neutron and gamma detection equipment, and analytic tools to evaluate the effectiveness of that equipment to detect nuclear materials of interest. NDFOM software computes the interaction of source and background radiation with detectors, and computes the detection likelihoods based on processing the signals generated by the detector. Medium-resolution detector materials such as Cadmium-Zinc-Telluride (CZT), and low-resolution detector materials such as Cesium-Iodide (CsI) and Sodium-Iodide (NaI), though unable to resolve individual lines in the incident spectral flux, allow the use of multiple-channel signal processing algorithms that can significantly outperform simpler total count algorithms. Even very-low-resolution materials like polyvinyl toluene (PVT) have some power to distinguish incident gammas of different energies. This document presents the methodology used in NDFOM to estimate the number of counts in detection energy channels, given the incident spectral flux, while accounting for the response of various detector materials.

During a scan, a detector records the number of counts in each of several energy channels. In the absence of a radiating source, the average background count in channel i is designated B_i. The variation in the background counts is typically quantified by the standard deviation of the observed background counts. In the presence of a radiating source, the detector will record S_i additional counts in energy channel i during a scan. The

[1] http://dtrandfom.lanl.gov/NDFOM, limited access.

simple total-count signal-to-noise figure-of-merit is the total source count divided by the standard deviation of the total background count:

$$snr_{total-count} = \sum_i S_i / \sqrt{\sum_j B_j} \quad (1)$$

A multi-channel matched-filter signal-to-noise processing approach can improve the effective signal-to-noise ratio to

$$snr_{multi-channel} = \sqrt{\sum_i S_i^2 / B_i} \quad (2)$$

Several figures-of-merit can be estimated based on the signal-to-noise ratio. One useful figure-of-merit is the probability of detection of a source for a specified false positive rate.

NDFOM constructs a non-uniform channel energy structure for use in equation 2. The channel energy widths are smaller at lower energy, and increase in proportion to the square root of the channel energy. CZT requires narrower channel widths than CsI or NaI, and PVT uses wider channels than the other materials. The high-resolution incident spectral fluxes are aggregated into a vector of incident flux in each channel. NDFOM constructs a detector response function matrix R to transform the incident gamma flux vector into a vector of detector counts per (m^2 s) in each channel. The matrix element R_{ji} gives the number of detections in energy channel j per incident gamma in energy channel i.

The number of detector counts per (m^2 s) is converted to number of detector counts in each energy channel by accounting for the detector area, the scan time, the detector thickness, any shielding or collimation structure that may be present, and possible motion of the source or the detector during the scan.

2 Background Spectral Fluxes

NDFOM provides two background gamma spectral flux distributions[2], shown in Figure 1. The gamma background flux is 3.79 γ/(cm² s) above 50 keV. More than half of the background gammas have particle energy between 100 and 300 keV.

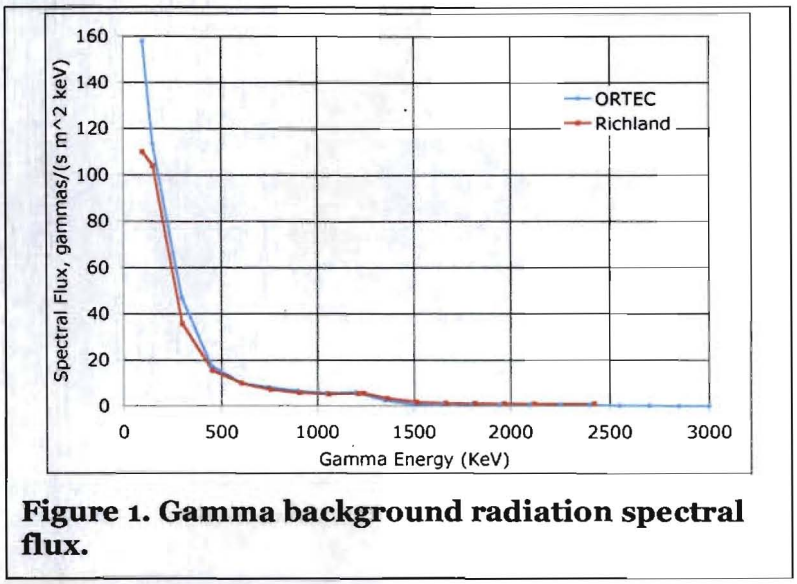

Figure 1. Gamma background radiation spectral flux.

A series of long-sample measurements[3] of mid-latitude environmental neutron flux reported 100±20 neutrons per (m² s). 30% of the neutron flux consisted of thermal neutrons with energy less than 0.5 eV. The epithermal flux (roughly following a 1/E dependence over the range 0.5 eV to 100 keV) and fast neutron flux (more than 100 keV) each make up 35% of the total flux. The background neutron flux is implemented in NDFOM by specifying the thermal, epithermal, and fast flux components.

3 Source Spectra

3.1 Unshielded Uranium-235

NDFOM provides a uranium-235 spectrum based on 25 kg of highly enriched uranium (HEU) composed of 93% ^{235}U and 7% ^{238}U. ^{235}U alpha decays with a specific activity[4] of 8.02x10⁴ Bq/g. 57.2% of ^{235}U decays are accompanied by emission of a 185.7 keV gamma. In addition, ^{235}U generates roughly 50 gamma lines at lower intensities. The 23.25 kg of ^{235}U in 25 kg of HEU generates 1.07x10⁹ γ /s of 185.7 KeV gammas.

---

[2] P. Bossew, *A very long-term HPGe-background gamma spectrum*, Applied Radiation and Isotopes, Vol 62, Issue 4, April 2005, pp. 635-644.

[3] M. Florek, J. Masarik, I. Szarka, D. Nikodemova, A. Hrabovcova, *Natural Neutron Fluence Rate and the Equivalent Dose in Localities with Different Elevation and Latitude*, Radiation Protection Dosimetry, Vol. 67, No. 3, pp. 187-192 (1996). Nuclear Technology Publishing.

[4] specific activity=ln(2) * Avogadro's number/mass number/half-life. 1 Becquerel (Bq) = 1 decay per second.

^{238}U undergoes alpha decay to ^{234}Th with a specific activity of 1.25×10^4 Bq/g. The ^{234}Th daughter immediately beta-decays to ^{234m}Pa, a meta-stable isotope of protactinium. The ^{234m}Pa emits a 1001.0 keV gamma (0.842% yield), in addition to many other gamma lines at lower relative intensities. The 1750 g of ^{238}U in 25 kg of HEU emits 1.84×10^5 γ/s of 1001.0 keV gammas.

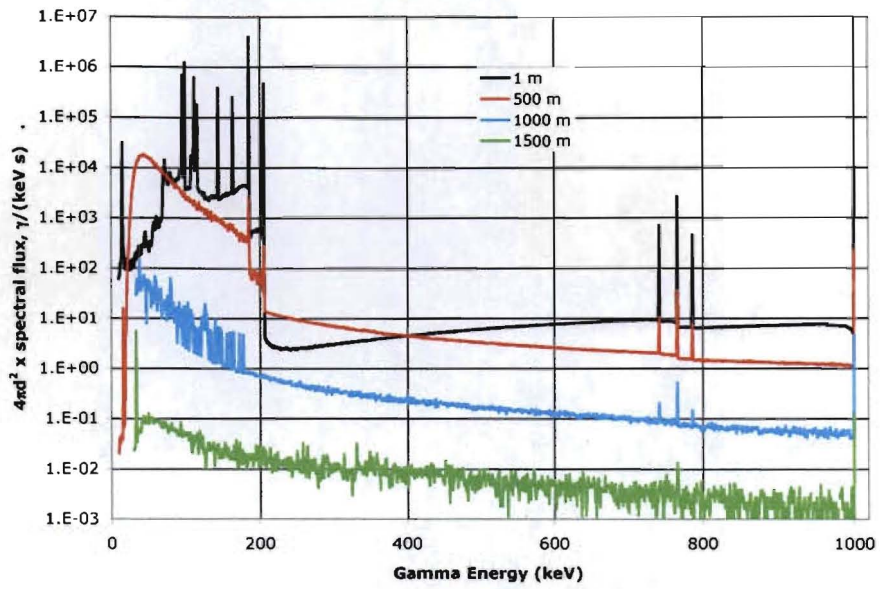

Figure 2. MCNP computed spectral flux from HEU source (multiplied by $4\pi d^2$), at 1, 500, 1000, and 1500 meters from the source. The total flux at 1 meter is 66.3 γ/(cm² s).

Figure 2 shows the flux (multiplied by $4\pi d^2$) in γ/(s keV) from a 25 kg HEU sphere as computed by MCNP-X simulations[5]. The fluxes are tallied at distances d of 1, 500, 1000, and 1500 meters from the source.

The MCNPX-simulated HEU total gamma flux from 0 to 1001 keV, at a distance of 1 meter from the HEU source, is 66.3 γ/(s cm²). 97% of the HEU gamma flux is in gammas with energy between 96 keV and 206 keV. In comparison, the gamma background flux is about 2 γ/(s cm²) in the 96 to 206 keV band.

In NDFOM, the source spectral flux at distance *d* from the source is interpolated from these MCNPX computations. 10 meters distant from the source, the flux drops to 0.592 γ/(s cm²), which breaks out into a factor of 100 for inverse square distance scaling, and a 0.89 factor due to air attenuation and build-up over 9 meters.

Although HEU produced by enrichment of natural uranium contains no ^{232}U, HEU derived from reactors does contain trace amounts of ^{232}U, typically at a few parts per billion ^{232}U or less. The seventh daughter in the ^{232}U decay chain is ^{208}Tl, which emits a 2614 keV gamma. If the HEU in question contains ^{232}U, this highly penetrating gamma could be brighter than the gammas emitted by ^{235}U and ^{234m}Pa. NDFOM also provides HEU spectra with low and moderate assays of ^{232}U.

The exposure rate is an energy integral over the spectral flux, given by

$$\dot{X}[\mu R/h] = 0.0663 \int dE\, \phi(E)\, E\, [1 - \exp(-\mu_{en-air})] / \rho_{air}$$

[5] MCNP-X simulations run at LANL by Laurie Waters and Joe Durkee.

where $\dot{X}$ is the exposure rate in μR/h, $\phi(E)$ is the spectral flux in $\gamma/(cm^2\ s\ keV)$, E is the gamma energy in keV, ρ_{air} is the density of air (0.00129 g/cm³), and $\mu_{en\text{-}air}$ is the energy attenuation coefficient for gammas in air. At 1 meter from a 25 kg unshielded HEU source, the exposure rate is 17.7 μR/h, little higher than the background exposure rate.

3.2 Shielded uranium-235 Source

A 5 mm thick lead shield can reduce the flux of 96 to 206 keV gammas (which make up the bulk of HEU gamma emissions) by factor of 1000, so we are interested in evaluating detector performance against shielded sources. NDFOM uses an attenuation and build-up method to compute gamma spectral flux for various thicknesses of lead shielding and various air propagation distances. The uncollided spectral flux at 1 meter from the source is given by

$$\phi_{uncollided}(E) = \phi_{unshielded}(E)\exp[-\mu_{Pb}(E)x]$$

where $\phi_{unshielded}(E)$ is the unshielded spectral flux at 1 meter from the source in $\gamma/(cm^2\ s\ keV)$, $\mu_{Pb}(E)$ is the energy-dependent attenuation coefficient in lead in cm^{-1}, and x is the lead shield thickness in cm. The attenuation coefficient is obtained by multiplying the mass attenuation coefficient in lead by the density of lead (11.34 g/cm³).

NDFOM models that the flux of collided gammas, $\phi_{collided}$, is given in terms of the build-up factor in lead, B(X,E), by

$$\phi_{collided}(E) = s(E)\cdot \int_{E}^{E_{max}} dE' \frac{\phi_{uncollided}(E')[B(\mu_{Pb}(E')x, E') - 1]}{\int_0^{E'} dE'' s(E'')}$$

where $X = \mu_{Pb}(E)x$ is the number of attenuation lengths, E is the gamma energy in keV, and s(E) is the normalized spectrum of the collided gammas. The outer integral accounts for down-scattering in energy from energies above E. The integral in the denominator truncates the normalized collided spectrum to energies below the initial energy of the scattering gamma. The Taylor formulation for the buildup factor is given by

$$B = A_1 e^{-a_1 X} + (1 - A_1)e^{-a_2 X}$$

where X is the number of attenuation lengths through which the radiation has passed[6]. We have fit the Taylor parameters for lead to the tabulation by Wallace[7], by A_1=0.003E, a_1=-0.035, and a_2 = 150/E, with E in keV.

The normalized spectrum of the collided spectrum was constructed from the spectral flux at 500 meters from an unshielded HEU source that was computed by MCNP, seen in Figure 2. The HEU gamma lines were removed from this spectrum, then the remaining collided spectrum was corrected to make it piecewise continuous between these

---

[6] A. Fodoraro, *The Photon Shielding Manual*, 2nd ed., Penn State Press.

[7] O. J. Wallace, "Gamma-ray dose and energy absorption build-up factor data for use in reactor shield calculations", Bettis Atomic Power Laboratory report WAPD-TM-1012, 1974.

gamma lines, and finally the result was normalized. The resulting normalized collided spectra is shown in Figure 3. A nearly identical normalized collided spectrum was obtained from an MCNP simulation of the gamma spectrum from plutonium, described below.

The total spectral fluxes including uncollided and collided gammas are shown in Figure 4, for lead shield thicknesses of 0, 1 mm, 5 mm and 2.5 cm.

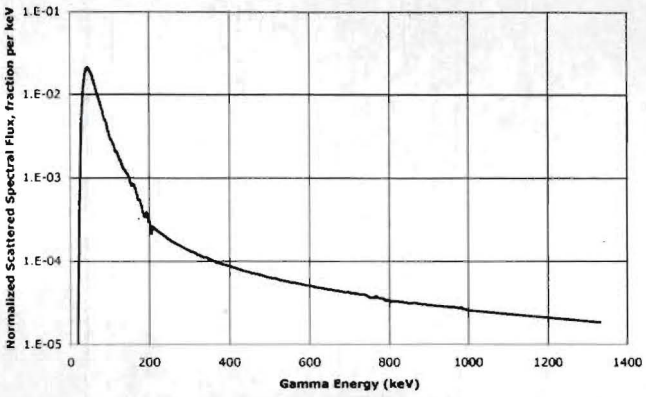

Figure 3. The normalized spectral flux of the scattered component from a 1332 keV primary gamma source, computed by MCNPX at 3.3 attenuation lengths from the source.

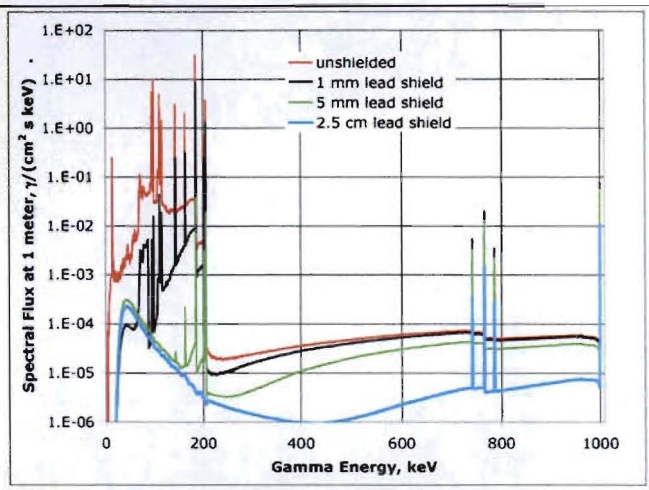

Figure 4. Gamma spectral fluxes from 25 kg HEU with 0, 1 mm, 5 mm, 2.5 cm thick lead shielding.

A 5 mm lead shield reduces the total gamma flux at 1 meter by a factor of 0.00243 from 66.3 to 0.161 γ/(cm² s). The flux of 185.7 keV gammas is reduced by a factor of 0.00116, while the 1001 keV gamma flux is only reduced by a factor of 0.669.

3.3 Plutonium-239

The IAEA uses 8 kg as the "significant quantity" of weapons-grade plutonium (wgPu), which consists primarily of the fissile isotope ^{239}Pu. We take a wgPu composition of 93.77% ^{239}Pu, 5.9% ^{240}Pu, 0.24% ^{241}Pu, 0.06% ^{241}Am, 0.2% ^{242}Pu, 0.01% ^{238}Pu, and trace amounts (initially 0.5 ppb) of ^{236}Pu leading to ^{208}Tl. Three isotopes emit detectable gammas (^{239}Pu, ^{241}Pu, and ^{236}Pu). ^{240}Pu emits spontaneous fission neutrons. Additional neutrons come from fission multiplication.

The 7.5 kg of ^{239}Pu in 8 kg of wgPu gives an activity[8] of 1.72×10^{13} Bq, which equates to 2.53×10^{8} γ/s of 413.713 keV gammas. Other gamma energies are generated with lower intensities.

^{241}Pu undergoes beta decay to ^{241}Am, which undergoes alpha decay. 35.9% of ^{241}Am decays are accompanied by emission of a 59.5 keV gamma and some higher energy gammas at low intensity. If the initial composition of ^{241}Pu was 0.3%, the ^{241}Am concentration would build to 0.06% after 4.6 years, which would generate 2.18×10^{11} gammas per second.

[8] www.nndc.bnl.gov/nudat2

^{236}Pu undergoes a series of decays that include the gamma-emitting daughters ^{212}Pb and ^{208}Tl. The ^{208}Tl emits a 2615 keV gamma, among others, and the ^{212}Pb emits a 238 keV gamma.

MCNP-X simulations run at LANL computed the gamma spectral flux from an 8 kg wgPu sphere. The spectral flux, in gammas per (s cm^2 keV) is shown in Figure 5, at 1 meter from the source. The total gamma flux at 1 meter is 6898 γ/(cm^2 s), roughly 100 times the flux from a 25 kg HEU source. More than 80% of the gammas emitted by this wgPu source are weakly-penetrating 59.5 keV gammas emitted by ^{241}Am.

MCNP-X was also used to simulate the neutron flux from an 8 kg wgPu sphere at distances of 1, 5, 10, 50, 100, 500, 1000, and 1500 meters from the source. The computed flux is tabulated in 201 logarithmic energy channels up to 19 MeV. The outward spectral flux (multiplied by 4π d^2) is shown in Figure 6.

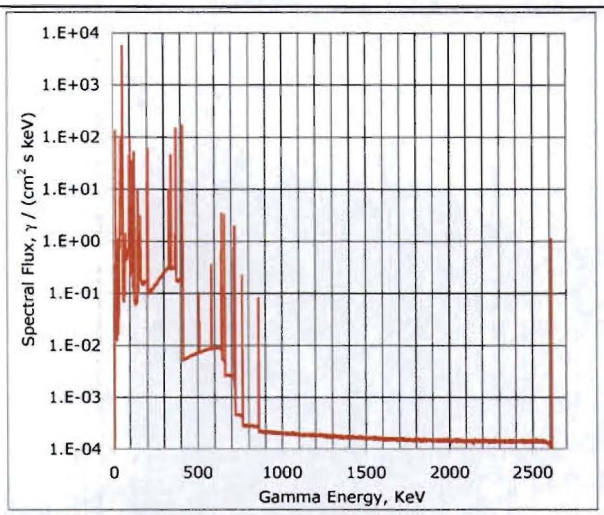

Figure 5. The gamma spectral flux 1 m from an 8 kg wgPu shell.

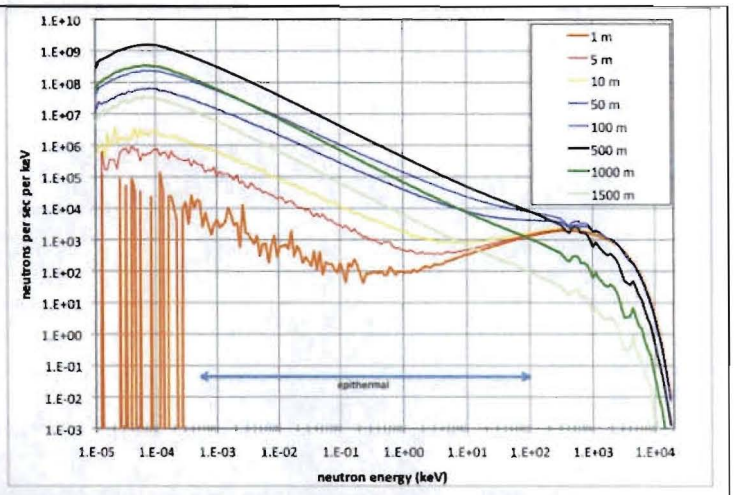

Figure 6. The outward neutron spectral flux times $4\pi d^2$ computed by MCNPX for 8 kg wgPu (n per second per keV).

The outward neutron spectral flux, ϕ, from a radiating source is implemented in NDFOM as a tabulation of $4\pi d^2\phi$ at a set of distances, for three energy groups. $4\pi d^2\phi$ represents the number of neutrons per second, in the given energy group, that would pass outward through a spherical surface of radius d. These fluxes are shown in Table 1, at various distances from the wgPu source.

	1 meter	5 meters	10 meters	50 meters	100 meters	500 meters	1000 meters	1500 meters
Thermal	8.25E+00	2.03E+02	7.87E+02	1.97E+04	7.50E+04	4.66E+05	9.92E+04	9.43E+03
Epithermal 0.5 eV-100KeV	8.32E+04	9.98E+04	1.32E+05	7.51E+05	2.09E+06	5.40E+06	8.91E+05	8.01E+04
Fast > 100 keV	4.16E+06	4.28E+06	4.43E+06	5.48E+06	6.27E+06	2.96E+06	3.48E+05	2.91E+04

Table 1. Three group outward neutron flux times $4\pi d^2$, from 8 kg wgPu source. Units are neutrons per second per group.

The total outward neutron flux at a distance of 1 meter from the source is 33.7 n/(s cm^2), primarily fast neutrons. This drops to 0.020 n/(s cm^2) at a distance of 50 meters, which is still double the flux of environmental neutrons.

3.4 Cobalt-60

^{60}Cobalt decays by beta decay with half-life 5.27 years to ^{60}Ni, which then emits a 1173.2 keV gamma followed immediately by a 1332.5 keV gamma. The specific activity is 1130 Ci/g. NDFOM takes 2 kCi as a nominal cobalt source activity. At 1 meter, in the absence of shielding, the flux is of 1.18×10^9 $\gamma/(cm^2\ s)$. At this flux, the exposure rate would be 2600 R/h at 1 meter, which requires shielding for handling or transportation.

The US Nuclear Regulatory Commission regulates external radiation standards for all packages intended for shipment. Title 10 Code of Federal Regulations part 71.47(a)[9] specifies that each package of radioactive materials offered for transportation must not exceed 200 mR/h on the external surface of the package. The shielding thickness of lead that reduces the source radiation from a 2 kCi 60Co source to 200 mR/h is found[10] to be 21.8 cm.

NDFOM applies an attenuation and buildup algorithm to compute the gamma spectra after the two emitted lines pass through the lead shield and intervening air. Applying the build-up factor formulation for lead described in Section 3.2, the build-up factors in the lead shield are 5.663 and 5.885, respectively.

NDFOM uses a polynomial formulation for the build-up factor in air:

$$B(X,E,air) = 1 + c_1 X + c_2 X^2$$

The polynomial coefficients are fit to the data of Wallace, where for air, $c_1 = 0.913(E/500)^{0.1485}$ and $c_2 = 0.4456(E/500)^{-0.1897}$. The spectrum of the collided gammas is taken to follow the collided spectrum shown in Figure 3.

The spectral flux multiplied by $4\pi d^2$ is shown in Figure 7, at distances of 1, 500, 1000, and 1500 meters from the shielded 2 kCi cobalt-60 source. The total (scattered and uncollided) flux 1 meter from the source is 3791 $\gamma/(cm^2\ s)$.

---

[9] http://www.nrc.gov/ reading-rm/doc-collections/cfr/part071/part071-0047.html
[10] www.radprocalculator.com

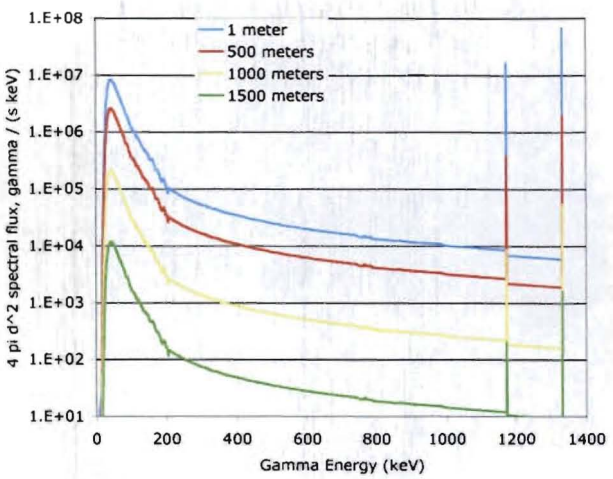

Figure 7. The spectral flux (multiplied by $4\pi d^2$) from a shielded 2 kCi cobalt-60 source, at distances of 1, 500, 1000, and 1500 meters.

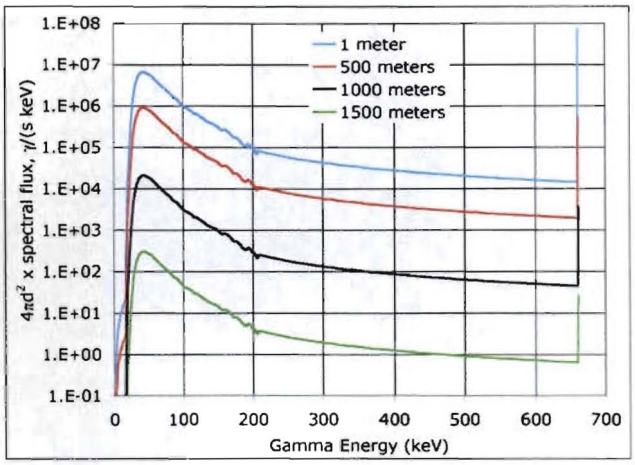

Figure 8. Spectral flux (times $4\pi d^2$) from 2kCi ^{137}Cs source with 10.85 cm lead shielding, at 1, 500, 1000, and 1500 meters.

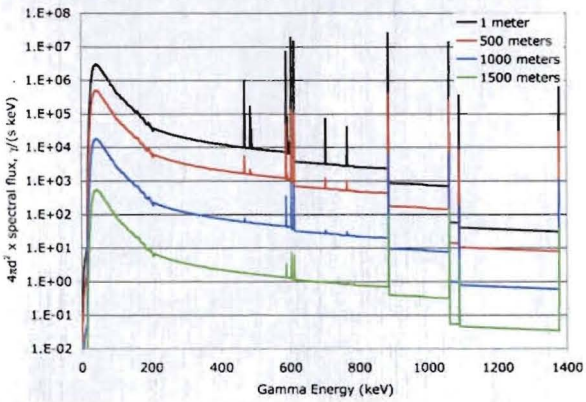

Figure 9. Spectral flux times $4\pi d^2$ from a 200 Ci ^{192}Ir source with 7.41 cm lead shielding, at 1, 500, 1000, and 1500 meters.

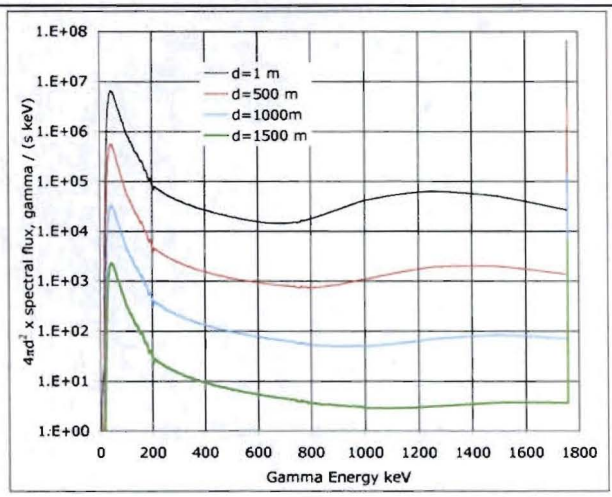

Figure 10. Spectral flux times $4\pi d^2$ from a shielded 15.9 kCi ^{90}Sr source, at distances of 1, 500, 1000, and 1500 meters.

3.5 Cesium-137

The specific activity of ^{137}Cs is 87 Ci/g. 94.6% of ^{137}Cs decays are beta decay to ^{137}Ba, and 89.9% of the resulting ^{137}Ba emits a 661.6 keV gamma. A 2 kCi ^{137}Cs source thus emits 6.29 10^{13} γ/s. This gamma source gives a flux of 5.01x10^{8} γ/(cm² s) and a corresponding exposure rate of 642.9 R/h at 1 meter from the source.

A 10.85 cm thick lead shield would reduce the exposure rate of a 2 kCi ^{137}Cs source to 0.2 R/h at the shield surface. An attenuation and build-up analysis was performed to compute the uncollided and scattered flux after propagation through the lead shield and air. The spectral flux composed of the uncollided 661.6 keV gamma and the scattered

component (both multiplied by $4\pi d^2$) is shown in Figure 8, at distances of 1, 500, 1000, and 1500 meters from the shielded 2 kCi ^{137}Cs source. The total (scattered and uncollided) flux 1 meter from the source is 3048 $\gamma/(cm^2\ s)$.

3.6 Iridium-192

Of the 61 domestic cases of stolen or lost radioisotopes sufficient to build an radiological dispersal device recorded by the Nuclear Regulatory Commission[11] for 1994 through 2005, the majority were ^{192}Ir. The notional ^{192}Ir source strength in NDFOM is 200 Ci. Handling this source without shielding would deliver a lethal dose (LD-50) of 500 rem in a few minutes. A lead shielding container 7.41 cm thick would reduce the surface exposure rate to 200 mR/h.

^{192}Ir decays with a half-life of 74.4 days, so the activity decreases by a factor of 30 per year. 96% of decays are beta decay to ^{192}Pt, and 4% of decays are electron conversion to ^{192}Os. The excited platinum and osmium nuclei emit several gammas. NDFOM uses the energy and yield of 41 gamma lines tabulated in NUDAT2[12]. The highest yield lines are 316.5 keV (82.71% yield), 468.07 keV (47.81% yield), 308.45 keV (29.68% yield) and 295.96 keV (28.72% yield). Higher energy gammas, though they are emitted with much lower relative intensity, are included because they are much less reduced by shielding or air propagation. There are a total of 2.352 gammas emitted per disintegration.

The gamma flux at 1 meter from an unshielded 200 Ci ^{192}Ir source is 1.35×10^8 $\gamma/(cm^2\ s)$, including the attenuation and build-up due to propagation through air. The flux from an unshielded 200 Ci ^{192}Ir source gives an exposure rate of 95.5 R/h at a distance of 1 meter from the source. A 7.41 cm thick lead shield will reduce the exposure rate at the shield surface to the package limit of 0.2 R/h. Figure 9 shows the spectral flux at 1 meter from a shielded 200 Ci ^{192}Ir source. The spectra are given as the product of $4\pi d^2$ times the spectral flux, at distances d of 1, 500, 1000, and 1500 meters from the source. These spectra include the attenuation and build-up due to propagation through the 7.41 cm lead shield and through air. The gamma flux 1 meter from the shielded source is 1740 $\gamma/(cm^2\ s)$.

3.7 Strontium-90

^{90}Sr was used as the power source in radioisotope thermoelectric generators. Many RTG's were used to power lighthouses in the Soviet Union in the 1970's, and have since been abandoned. These sources are typically 5 kg cylinders, 10 cm in height and diameter. Originally, they were 35 kCi, but have decayed to ~15.9 kCi (33 years, at a half-life of 28.9 years).

^{90}Sr decays by beta decay to ^{90}Y, which rapidly decays by another beta decay. 0.0115% of ^{90}Y decays are accompanied by emission of a 1760.7 keV gamma [NUDAT2]. Since the half-life of the ^{90}Sr decay (29.1 years) is much greater than that of the ^{90}Y decay (64 hours), the activity of both decays are essentially identical. A 15.9 kCi source generates 1.17×10^{15} betas per second, and 6.77×10^{10} 1760.7 keV gammas per second. The beta particles are stopped close to their point of origin. In the stopping process, the beta particles (electrons) collide with electrons in the stopping material, emitting bremsstrahlung radiation.

---

[11] Steve Coll, "The Unthinkable", New Yorker, March 12, 2007

[12] http://www.nndc.bnl.gov/nudat2/

Yaar[13] published a measurement of the bremsstrahlung gamma spectrum from a $^{90}Sr/^{90}Y$ source. The detected gamma counts per second per keV were published for the case of a 0.1622 Ci source, using a 7.5 cm x 7.5 cm x 7.5 cm NaI detector placed 30 cm from the source, with shielding between the source and detector consisting of 0.5 mm steel, 3 mm lead, and 1 mm copper. We scale the source strength to 15.9 kCi, scale the distance to 1 meter, and divide Yaar's counts per second by the NaI detection efficiency as a function of energy to obtain the gamma spectral flux at 1 meter from a 15.9 kCi $^{90}Sr/^{90}Y$ source. The total flux is 3.40×10^7 $\gamma/(cm^2\ s)$, including 4.28×10^5 $\gamma/(cm^2\ s)$ from the gamma line at 1760.7 keV. It includes the effect of the three layer shield, and because Yaar's results are for a very small source, there is no self shielding effect.

NDFOM uses an attenuation and buildup formulation to add the effect of self shielding. The self attenuation as a function of energy is given by

$$\chi(E) = \{1 - \exp[-(\mu/\rho)_{Pb}\rho_{SrTiO_3}x)]\} / [(\mu/\rho)_{Pb}\rho_{SrTiO_3}x]$$

where $(\mu/\rho)_{Pb}$ is the mass attenuation coefficient in lead, ρ_{SrTiO_3} is the density of the strontium material (5.12 g/cm^3) and x is the effective path length due to self shielding. For consistency with Yaar's results, the effective path length due to self shielding is 5.27 cm, which gives a reduction factor of 0.165 in total flux due to self shielding. The effective number of attenuation lengths, X, due to self shielding for use in calculating the buildup of scattered gammas is taken to be

$$X(E) = -\ln(\chi(E))$$

The build-up factor in lead as a function of energy and number of attenuation lengths is as described in 3.2. The scattered gamma flux is obtained by multiplying the uncollided flux by B-1, and the total flux is given by the sum of the collided and uncollided flux.

Next, we performed an inverse buildup calculation to remove the effect of Yaar's three-layer shield. The total flux at 1 meter is 2.22×10^7 $\gamma/(cm^2\ s)$, of which 2.99×10^5 $\gamma/(cm^2\ s)$ is from the ^{90}Y line at 1760.7 keV. There are 0.0024 bremsstrahlung gammas emitted per beta particle.

The gamma flux from an unshielded strontium source would generate an exposure rate far in excess of the transportation package limit. Therefore, we computed the thickness of lead that would be required such that the exposure rate at the package surface would be reduced to 0.2 R/h, including buildup of scattered gammas. We find that 11.5 cm of lead is required for this exposure rate reduction.

The effect of attenuation and build-up on the gamma spectrum due to propagation through various distances in air were computed to give the spectral fluxes in a form suitable for use in NDFOM. The spectral fluxes, multiplied by a factor of $4\pi d^2$, are shown at distances d of 1, 500, 1000, and 1500 meters from the source in Figure 10, including self shielding and shielding from a 11.5 cm thick lead shield. The total flux at 1 meter is 4310 $\gamma/(cm^2\ s)$, of which 397 $\gamma/(cm^2\ s)$ are uncollided 1760.7 keV gammas from ^{90}Y, 702 $\gamma/(cm^2\ s)$ are uncollided bremsstrahlung gammas, and 3210 $\gamma/(cm^2\ s)$ are scattered gammas.

---

[13] I. Yaar and E. M. A. Hussein, Passive detection of concealed strontium-90 radioisotope thermoelectric generators in transport, RAMTRANS, vol. 15, No. 2, pp. 149-154 (2004).

3.8 Plutonium-238

280 Ci ^{238}Pu sources were used in radioisotope thermoelectric generators. ^{238}Pu material is created in reactors. The resulting plutonium product consists of a mix of plutonium isotopes[14], with isotopic fractions as shown in Table 2. Three of these isotopes are significant gamma emitters: ^{238}Pu, ^{241}Pu and ^{236}Pu.

isotope	Isotope fraction in product
^{238}Pu	81%
^{239}Pu	15%
^{240}Pu	2.9%
^{241}Pu	0.8%
^{242}Pu	0.1%
^{236}Pu	0.00012%

Table 2. Isotopic composition of manufactured "plutonium-238" material.

A 280 Ci "fresh plutonium-238" product contains 20.168 g of plutonium, of which 16.336 g is ^{238}Pu. ^{238}Pu emits 36 gamma lines. 280 Ci of ^{238}Pu emits 2.28 x10^6 γ/s of 766.39 keV gammas. The emission rate of these 766.39 keV gammas drops exponentially with time, following the 87.7 year half-life of ^{238}Pu.

^{238}Pu also undergoes spontaneous fission (yield of 1.9x10^{-9} per disintegration), which is accompanied by emission of neutrons and gammas. The spontaneous fission rate of 280 Ci of ^{238}Pu is 19,684 per second, giving 45,860 neutrons/s, and approximately 180,000 γ/s. These gammas are distributed in energy with an average energy of ~800 keV. The emission rate of these spontaneous fission gammas is thus only 5% of the emission rate of penetrating gammas associated with alpha decay.

A 280 Ci "plutonium-238" source contains 0.0242 mg of ^{236}Pu. ^{236}Pu undergoes a series of 9 transitions, ending with stable ^{208}Pb. The chain dynamics are controlled by the first three α–decay transitions: ^{236}Pu to ^{232}U with 2.858 year half-life, then ^{232}U to ^{228}Th with 68.9 year half-life, then ^{228}Th decay with 1.92 year half-life. The remaining transitions have relatively short half-lives, so their activity is essentially equal to that of ^{228}Th. In a 280 Ci ^{238}Pu source, the activity of ^{228}Th in Bq as a function of time t in years is given by

$$A_{Th228} = \left[\frac{\tau_{Pu236} e^{-t \ln(2)/\tau_{Pu236}}}{(\tau_{Pu236} - \tau_{Th228})(\tau_{Pu236} - \tau_{U232})} + \frac{\tau_{U232} e^{-t \ln(2)/\tau_{U232}}}{(\tau_{Th228} - \tau_{U232})(\tau_{Pu236} - \tau_{U232})} + \frac{\tau_{Th228} e^{-t \ln(2)/\tau_{Th228}}}{(\tau_{Pu236} - \tau_{Th228})(\tau_{Th228} - \tau_{U232})} \right] \frac{N_0^{Pu236} \ln(2)}{31{,}557{,}600}$$

where τ_i is the half-life of isotope i in years, and N_0^{Pu236} is the number of ^{236}Pu nuclei in a freshly manufactured 280 Ci source ($N_0^{Pu236} = 6.124 \times 10^{16}$). The ^{228}Th activity builds up to a maximum of 1.677x10^7 Bq, attaining this maximum activity 17.8 years after manufacture.

Two of the daughter isotopes in the ^{236}Pu decay chain emit γ radiation. ^{212}Pb, the 6th daughter in the chain, emits 0.436 gammas per disintegration of ^{228}Th, with gamma energy of 238 keV. ^{208}Tl, the 8th daughter in the chain is created in 35.94% of ^{228}Th decays.

---

[14] George M. Matlck and Charles F. Metz, Radiation Characteristics of Plutonium-238, Los Alamos Scientific Laboratory report LA-3696 (1967).

^{208}Tl emits four penetrating gammas: 99.7% of decays ^{208}Tl decays emit a 2614 keV gamma, 12% emit an 860 keV gamma, 85% emit a 583 keV gamma, and 22% emit a 510 keV gamma.

The ^{241}Pu in the manufactured product decays with a 14.35 year half-life to ^{241}Am, which emits a 59.54 keV gamma with a 35.9% yield. The emission rate builds to 2.82x10^{9} γ/s in 10 years, and reaches a maximum rate of 6.05x10^{9} in 70 years.

The spectral gamma flux is shown in Figure 11 at a distance of 1 meter from a 10 year old 280 Ci 238Pu source, accounting for the three isotopes described above. The total flux at 1 meter is 2.46x10^{4} γ/(cm^{2} s).

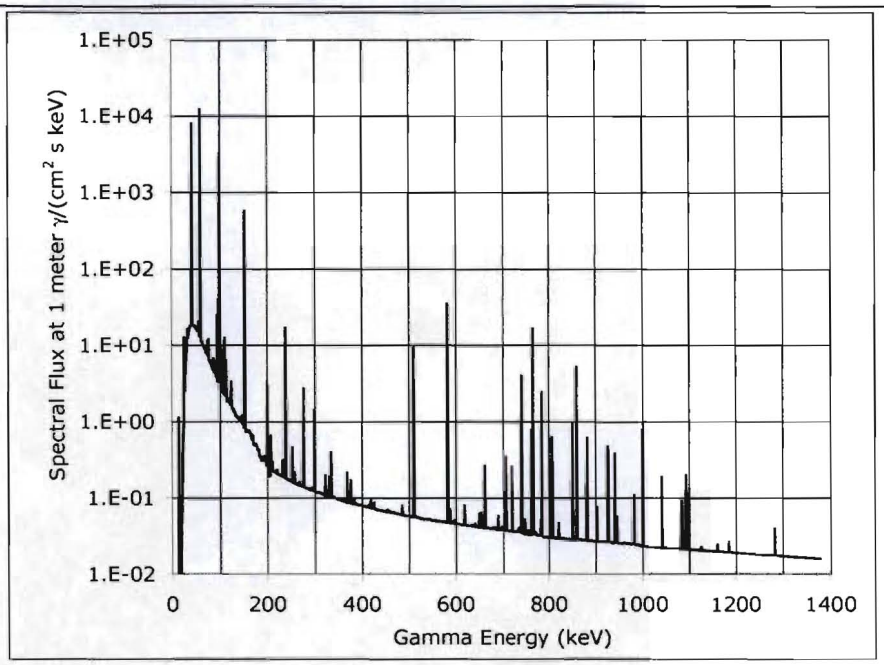

Figure 11. Spectral flux 1 meter from a 10 year old 280 Ci 238Pu source, γ/(cm^{2} s keV).

The neutron flux in thermal, epithermal, and fast groups as a function of distance is computed by scaling the fluxes computed for wgPu to a source strength of 45,900 n/s, and are tabulated in Table 3.

	1 meter	500 meters	1000 meters	1500 meters
Thermal	0.3	1371	229	2.6
Epithermal 0.5 eV to 100KeV	835	12,776	1766	25.4
Fission spectrum	45,060	6287	651	23.1

Table 3. Neutron group fluxes (times 4πd^{2}), in n/s, from 280 Ci plutonium-238 source.

3.9 Americium-241.

Americium-241 is of interest because it is a daughter of the ^{241}Pu in wgPu and in plutonium-238 material, but it is also of interest because of its use in AmBe neutron

sources. ^{241}Am decays to ^{237}Np by alpha decay, with a half-life of 432.2 years, giving 1.27×10^{11} Bq/g. The excited ^{237}Np then emits gammas. 35.9% of decays emit a 59.5 keV gamma and 37% emit a 13.9 keV gamma [www.nndc.bnl.gov/nudat2]. Dozens of additional gamma and alpha lines are emitted, but with very low relative intensities.

A 20 Ci americium-241 source emits 2.55×10^{11} 59.5 keV gammas per second. The mass attenuation coefficient of 59.5 keV gammas in air is 0.1875 cm^2/g. The corresponding air-attenuated gamma fluxes are 2.06×10^6, 2.18×10^5, 1.66×10^4 γ/(cm^2 s) at 1, 3 and 10 meters, respectively. Using a lead mass attenuation coefficient of 5.131 cm^2/g, lead shielding of 0.5 cm, 1 cm, and 2 cm thickness would reduce the 59.5 keV gamma flux to 7115, 24.5, and 0.00029 γ/(cm^2 s) at 1 meter, respectively.

Well-logging sources use ^{241}Am combined with beryllium, in a mix with 13 beryllium atoms per americium atom. The emitted alphas undergo (α, n) reactions in the beryllium to generate the neutrons used for well logging. The neutron source rate[15] is 2.26×10^6 n/(s Ci). The neutron dose rate at 1 meter is 1.7 mrem/(hr Ci). For a well-logging source of 20 Ci, the neutron source rate is 4.52×10^7 n/s, and the neutron dose rate at 1 meter is 34 mrem/h. The neutron fluxes in thermal, epithermal, and fast neutron groups as a function of distance is computed in NDFOM by scaling the neutron fluxes computed for wgPu to a neutron source rate of 4.52×10^7 n/s. The neutron fluxes, times $4\pi d^2$, in neutrons per second per group, are listed in Table 4.

	1 meter	500 meters	1000 meters	1500 meters
Thermal	275	1350576	225962	2597
Epithermal 0.5 eV to 100KeV	821957	12581443	1739402	25056
Fission spectrum	4.437×10^7	6190651	641295	22764

Table 4. Three group neutron fluxes, times $4\pi d^2$, from 20Ci ^{241}Am neutron source.

3.10 Californium-252

^{252}Cf sources with activity of 37 mCi are used in well-logging equipment and conveyer gauges. ^{252}Cf decays with a half-life of 2.645 years, giving a specific activity of 536 Ci/g. A 37 mCi source is a grain 0.2 mm in diameter with a mass of 69 μg. 96.91% of disintegrations emit an alpha, but ^{252}Cf is primarily used as a source of neutrons. 3.09% of disintegrations are by spontaneous fission, each generating on average 3.76 neutrons and ~8 gammas of 800 keV average energy. The neutrons follow a Watt distribution with an average energy of 2.1 MeV. A fresh 37 mCi ^{252}Cf source emits 1.59×10^8 spontaneous fission neutrons per second.

At a distance of 1 meter, in the absence of shielding, a fresh 37 mCi ^{252}Cf source gives a fast neutron flux of 1266 n/(cm^2 s), well above the typical sea-level background fast neutron flux of 0.0035 n/(cm^2 s). The neutron flux from an unshielded 37 mCi 252Cf source is 269 times higher than that from an 8 kg shell of wgPu.

The neutron fluxes in thermal, epithermal, and fast neutron groups as a function of distance is computed in NDFOM by scaling the neutron fluxes computed for wgPu to a

[15] Erik F. Shores, Contact Dose Equivalent Rates from Common Neutron Sources, LA-UR-00-3092 (Sept 2000).

neutron source rate of 1.59×10^8 n/s. The neutron fluxes, times $4\pi d^2$, in neutrons per second per group, are listed in Table 4.

	1 meter	500 meters	1000 meters	1500 meters
Thermal	9.674E+02	4.751E+06	7.949E+05	9.136E+03
Epithermal 0.5 eV to 100KeV	2.891E+06	4.426E+07	6.119E+06	8.814E+04
Fission spectrum	1.561E+08	2.178E+07	2.256E+06	8.008E+04

4 MCNP Simulations of Gamma Detector Response Functions

Some incident gammas that enter the scintillator material in a detector will generate light that is in turn collected in a photomultiplier tube. The amount of light generated by a particular gamma particle is a stochastic variable that follows a distribution derived from the physics of the interaction of gammas with the material. By feeding the photo-multiplier output to a multichannel analyzer, the amount of energy deposited in the detector by each photon can be measured. The distribution of deposited energy can be calibrated by observing the distribution from a monoenergetic flux of gammas, often the 662 keV gammas emitted by a ^{137}Cs calibrating source.

4.1 Polyvinyl Toluene

The Monte Carlo neutron and gamma radiation transport code MCNPX was used[16] to compute the distribution of energy deposited by mono-energetic gammas incident on a 5 cm thick slab of organic (polyvinyl toluene) scintillator material. Ten incident gamma energy cases were run, from 100 keV to 1000 keV in 100 keV increments. An additional two cases were run with incident gamma energies of 2 and 3 MeV. For each run, the MCNPX output is a list of 1000 values, giving the fraction of incident gammas that deposit an energy in each of 1000 consecutive 1-keV-wide energy bins (3.0 keV and 3.5 keV-wide for the 2 MeV and 3 MeV runs, respectively). The fractions of incident gammas that deposit an energy in 1 keV about energy D are shown in Figure 12 for incident energies up to 1000 keV.

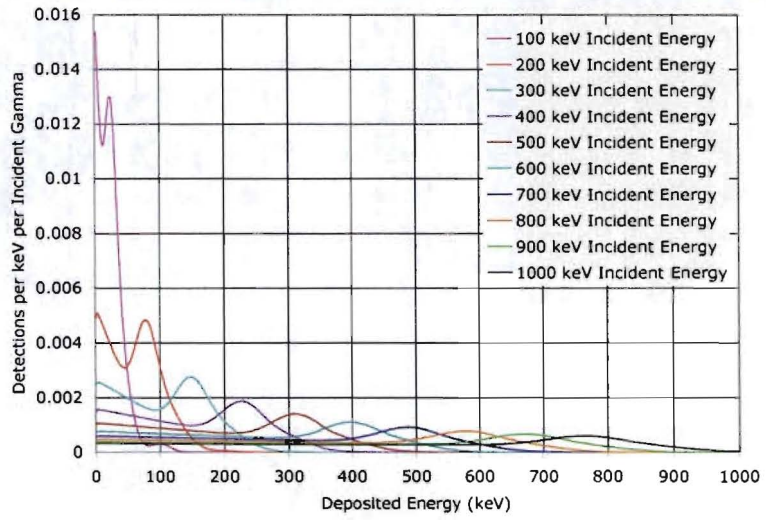

Figure 12. The fractions of incident gammas that deposit amounts of energy per keV, for incident gamma energies from 100 to 1000 KeV.

[16] MCNP-X simulations run by Laurie Waters and Joe Durkee of LANL.

The MCNPX-computed detector response functions for polyvinyl toluene each show an obvious main peak. In each case, the center energy of this peak is slightly below the Compton backscatter energy.

Taking the area of the main peak to be 1.064 times the product of the peak height and the FWHM[17] gives a main peak area of 0.118: that is, 11.8% of incident 1000 keV gammas would be detected in the main peak. Meanwhile 18.7% of incident 1000 keV gammas would be detected at lower energy, and the remaining 69.5% would pass through the material undetected.

The center energy of the main absorption peaks that appear in Figure 12 are tabulated in Table 5 for each MCNPX simulation of the PVT DRF. Also, the full-width-at-half-max of the main peak, and the detections per incident gamma in the main peak extracted from the detailed MCNPX simulations are tabulated. The FWHM is estimated as twice the half-width-at-half-maximum, by finding the energy at which f(D) takes a value of one half of f_p, by looking at how f(D) drops from its peak value as D increases above P. The area under the main peak, A, is estimated as the product of 1.064 f_p FWHM.

E incident energy, keV	Compton energy[18] keV	P center of main peak, keV	f_p main peak height, detections per keV per incident gamma	FWHM keV	Area of main peak detections per incident gamma
100	28.1	24	0.01299	30	0.415
200	87.8	79	0.004841	60	0.309
300	162.0	148	0.002751	88	0.258
400	244.1	227	0.001877	108	0.214
500	330.9	311	0.001405	126	0.186
600	420.8	397	0.001117	146	0.173
700	512.8	488	0.0009192	160	0.156
800	606.3	581	0.0007744	172	0.141
900	701.0	673	0.0006739	180	0.128
1000	796.5	767	0.0005889	188	0.118
2000	1773.4	1728	.000251	272	0.0726
3000	2764.6	2714	.000145	302	0.0466

Table 5. Main peak parameters for the DRF of PVT

4.2 MCNPX Simulations for Sodium Iodide

MCNPX was used to compute the detector response function of an NaI scintillator for ten incident gamma energies (100 keV, 200 keV, ..., 1000 keV). The DRF for each incident energy was output as the fraction of incident gammas that deposit an energy between D-1 and D keV, for D ranging from 1 to 1205 keV, in 1 keV increments. In all ten cases, the center energy of the main peak is equal to the incident gamma energy.

The center energy of the main absorption peaks are tabulated in Table 6 for each of MCNPX simulation of the NaI DRF. Also, the full-width-at-half-max of the main peak, and

---

[17] For a Gaussian peak, the peak area is given by

$$A = f_P \, FWHM \, \sqrt{\pi / (4 \ln(2))} = 1.064 \, f_P \, FWHM$$

[18] The most energy that can be deposited by a Compton scattering event is E/(1+511/2E), where E is the energy of the incident gamma in keV.

the detections per incident gamma in the main peak extracted from the detailed MCNPX simulations are tabulated.

E incident energy, keV	P center of main peak, keV	fp main peak height, detections per keV per incident gamma	FWHM keV	Area of main peak detections per incident gamma
100	100	0.04368	19	0.883
200	200	0.03102	27	0.891
300	300	0.02273	34	0.822
400	400	0.01665	40	0.709
500	500	0.01265	44	0.592
600	600	0.009922	50	0.528
700	700	0.008100	54	0.465
800	800	0.006727	58	0.415
900	900	0.005733	63	0.384
1000	1000	0.005031	67	0.359

Table 6. Main peak parameters for the MCNPX-computed detector response functions of a 5 cm thick NaI scintillator.

4.3 Cesium Iodide

A set of CsI DRF files was constructed from the MCNPX simulations of the NaI DRF's by applying an appropriate spread to the MCNPX-computed NaI DRF's. In all ten cases, the center energy of the main peak is equal to the incident gamma energy. The parameters of the DRF's that are required for DRF interpolation are tabulated in Table 7.

E incident energy, keV	P center of main peak, keV	fp main peak height, detections per keV per incident gamma	FWHM keV	Area of main peak detections per incident gamma
100	100	0.03616	24	0.923
200	200	0.02562	34	0.927
300	300	0.01864	42	0.833
400	400	0.01354	49	0.706
500	500	0.01035	55	0.606
600	600	0.00807	62	0.533
700	700	0.00660	67	0.471
800	800	0.00553	73	0.430
900	900	0.00469	78	0.389
1000	1000	0.00407	84	0.364

Table 7. Main peak parameters for CsI material DRF's.

4.4 Cadmium-Zinc-Telluride

Detectors made from Cadmium-Zinc-Telluride have intermediate resolving power, with a FWHM of 12-20 keV for gamma energy of 662 keV. CZT gamma detectors are used

in the Interceptor pager from Thermo Electron and the RadID handheld spectrometer from D-tect Systems. CZT crystals can only be grown in small sizes, typically less than a square cm in area and less than 1 cm thick.

The DRF for each incident energy is tabulated as the fraction of incident gammas that deposit an energy between D-1 and D keV, for D ranging from 1 to 1205 keV, in 1 keV increments. The center energy of the main peak is equal to the incident gamma energy. The parameters of the DRF's that are required for DRF interpolation are tabulated in Table 8.

E incident energy, keV	P center of main peak, keV	fp main peak height, detections per keV per incident gamma	FWHM keV	Area of main peak detections per incident gamma
100	100	0.1719	4.75	0.869
200	200	0.1227	6.75	0.881
300	300	0.0901	8.5	0.815
400	400	0.0661	10	0.703
500	500	0.0502	11	0.588
600	600	0.0394	12.5	0.524
700	700	0.0322	13.5	0.462
800	800	0.0267	14.5	0.412
900	900	0.0228	15.75	0.382
1000	1000	0.0200	16.75	0.356

Table 8. Main peak parameters for CZT material DRF's, based on a 5 cm thick detector.

5 Interpolation of Detector Response Functions

Each MCNPX computation requires 16 hours on a cluster of 10 processors (at 2.4 GHz). A practical approach to modeling the detector response function over a range of incident gamma energy requires a capability to interpolate detector response functions between a few detailed MCNPX computations.

The NDFOM detector response algorithm therefore applies an interpolation approach that ensures that the main peak varies smoothly as incident energy varies between incident energies of MCNPX runs. The idea is to interpolate the center energy and main peak area for incident gamma energies between the MCNPX case runs, and then to dilate and scale the bracketing MCNPX runs to match the interpolated main peak area and center, and then to take an appropriate linear combination of the two bracketing dilated-and-scaled MCNPX results.

5.1 Interpolation and Extrapolation of Main Peak Energy and Area

For a specified incident gamma energy, E, the algorithm first finds the MCNPX runs with the highest incident energy below E (designated E_{bot}), and the lowest incident energy above E (designated E_{top}). If E is less than the lowest incident energy in the set of MCNPX runs, E_{bot} will represent the lowest incident energy MCNPX case, and E_{top} will be the second lowest. Likewise, If E is more than the highest incident energy in the set of MCNPX runs, E_{bot} will represent the second highest incident energy MCNPX case, and E_{top} will be the highest. The corresponding MCNPX-computed peak energies and peak areas are designated P_{bot}, P_{top}, A_{bot}, and A_{top}. The interpolation formulas for the main peak center

energy P and the area under the main peak, A, for incident gamma energy E are given in equations 3 and 4.

$$P = P_{bot}\left(E/E_{bot}\right)^{\ln(P_{top}/P_{bot})/\ln(E_{top}/E_{bot})} \quad (3)$$

$$A = A_{bot}\left(E/E_{bot}\right)^{\ln(A_{top}/A_{bot})/\ln(E_{top}/E_{bot})} \quad (4)$$

5.2 Imputation of DRF

NDFOM imputes the number of detections per incident gamma, in a detection bin extending from D_1 to D_2 keV, for incident energy E, from MCNPX run n with incident energy E_n. Each MCNPX run generates a set of bin values, representing the number of detections in an detected energy range extending from (m-1) d to m d keV, per incident gamma, for incident energy E_n, where d is the MCNPX result detector bin width in keV for that run, and m is the detection bin number, extending from 1 up to the number of bins in that MCNPX run. The MCNPX output binwidth varies for different runs. The algorithm for imputing the DRF at an incident gamma energy of E from the DRF computed by MCNPX at an incident gamma energy of E_n is shown in the following pseudocode:

```
Pn = main peak energy for incident gamma energy of En
An = main peak area for incident gamma energy of En
P = interpolated peak energy for incident gamma energy of E
A = interpolated peak area for incident gamma energy of E
b = Pn / P                          # dilation factor
d = channel width for MCNP run at En, in keV
j1 = greatest integer less than (D1 * b / d)
j2 = greatest integer less than (D2 * b / d)
IF j1 >= len(f): RETURN 0.
IF j1 == j2 THEN RETURN f[j2][n]*(D2-D1)*b* A / An

# get the contribution from the first overlapping bin
g = f[j1][n]*A/An *((j1 + 1.0)* d - b*D1)

#  get the contributions from data bins that are entirely within
#  the dilated detection bin m
LOOP OVER j FROM j1+1 TO j2-1, inclusive
   if j > len(f)-1: RETURN g
   g += f[j][n] * d * A/An
END LOOP
#  get the contribution from the last overlapping bin
IF j2 < len(f) THEN g += f[j2][n] *A/An * (b*D2 – j2 * d)
RETURN g
```

where f[j][n] is a 2-D array holding the MCNPX-computed value of the number of detections per keV per incident gamma of energy E_n, at detection energy between j d and (j+1) d, and g is the imputed number of detections per incident gamma of energy E, in a

detection bin extending from D_1 to D_2 keV. Note that the j1==j2 block handles the case that the entire detection bin from D_1 to D_2 projects to one bin of the MCNPX result. A and P are computed with equations 3 and 4. Note also that this algorithm can impute the DRF to below the lowest MCNPX run and to above the highest MCNPX run, as long as the extrapolation of P and A are valid.

5.3 Linear Combination of Two Imputations

To extrapolate from the MCNPX runs to higher incident energy than the highest MCNPX run, or lower than the lowest MCNPX run, NDFOM imputes from the highest or lowest run only. If the incident energy E matches that of an MCNPX run, the imputed DRF simply equals the DRF from that single MCNPX run. However, when the incident energy E is bracketed by the incident gamma energy of two MCNPX runs, say E_{bot} and E_{top}, NDFOM computes the imputed DRF from both runs, and then obtains the DRF as a linear combination of the two imputed DRF's. The weight given to the DRF imputed from the MCNPX run with incident energy E_{top} is $z = (E-E_{bot})/(E_{top}-E_{bot})$. The weight given to the DRF imputed from the MCNPX run with incident energy E_{bot} is 1-z.

5.4 Dependence of Detector Response Function on Detector Thickness

Four sets of MCNPX runs were executed for the NaI scintillator. In all four cases, the detector face is 4 inches by 16 inches. The detector thickness of two of the sets was 5 cm, while the thickness in the other two sets was 10.0 cm. For both thicknesses, one set modeled normal incidence and the other modeled 45 degree incidence angle.

The overall detector efficiency for a given incident gamma energy is very well fit by a simple relation derived from exponential attenuation. The NDFOM incorporates the detector thickness into the detector response function computation through a multiplicative factor of $[1-(1-\eta)^{t/0.05}]/\eta$, where t is the detector thickness in meters, and η is the overall detection efficiency (that is, the sum over all detection energy bins) at a given incident gamma energy for a 0.05 meter thick detector. Note that the detector material thickness factor is a function of incident gamma energy.

6 Detector Response Function Matrix

6.1 Non-uniform Channel Energy Structure

From values derived from MCNPX runs, the FWHM of the main peak of the DRF is seen to be fairly well approximated as proportional to the square root of the main peak center energy, P. The appropriate channel energy structure for assessing multichannel signal to noise ratio consists of a sequence of channels with binwidth increasing as the square root of the energy. The bottom energy of the first channel, B[0], is given by the detector's minimum detectable energy threshold, which is typically 50 keV (as in the Ranger from Quantrad Sensor) or 60 keV (as in the RadEye PRD from ThermoElectron).

We find that the optimal filter, which makes use of all the resolution that a detector can provide, can be computed using a channel structure that has 2π channels spanning the FWHM resolution. This is the channel structure used to evaluate equation (2). Finer channel structure does not improve the calculation, but coarser channel structure introduces errors in the computed signal-to-noise.

For the NaI detector, this formulation gives 282 channels to span the detection energy and incident energy range from 50 keV to 2700 keV. The channels increase in width from 2.2 keV at 50 keV, up to 17 keV at 2700 keV.

For the PVT detector, this formulation gives 83 channels to span the 50-2700 keV range, with channel width varying from 7.7 keV to 55.7 keV. We note that if a uniform channel energy width of 7.6 keV were used instead of the non-uniform channel width, 343 channels would be required to compute the signal-to-noise with the same fidelity. The nonuniform channel energy width treatment reduces the DRF matrix size by a factor of 18, and provides a significant speed-up in the algorithm computation time.

6.2 Computation of the Detector Response Function Matrix Elements

For computation of detector performance, the NDFOM software computes a square matrix, R, based on the above channel energy structure. An incident spectral flux is expressed as a vector of channel fluxes: s[i] is the number of incident particles per (m^2 s) with energy between B[i] and B[i+1]. The matrix product of R with s gives a detected count vector, c, which is used directly in the computation of the matched filter signal to noise ratio. The matrix element R_{ji} is the number of detections in channel j per incident gamma in channel i.

We find that while it is critical to use the detailed data to perform the sum over the detection energy, it is much less critical to use the detailed data to perform the average over the incident energy. A simple sampling of incident energy values in energy bin i is sufficient. We find sampling the incident energy at every 6 keV produces the same accuracy as sampling at 1 keV steps, which results in a significant speed-up in the calculation. The DRF matrix is constructed with the following method of NDFOM's DetectorResponseFunction class:

```
def makeBlockKernel(self):
    b=self.snrBinEnergies
    self.speedUpFactor = 6.0
    numBins = len(b)-1
    ker=[]
    for n in range(numBins): # each incident energy bin
        samples = max(2,int( (b[n+1]-b[n])/self.speedUpFactor))
        deltaE= (b[n+1]-b[n])/float(samples)
        kerAcm=numBins * [0.0] # to hold the drf vector returned by interpolate2
        for i in range(energiesToAverage):
            e = int( b[n]+  (0.5+float(i)) * deltaE )
            kerInc= self.interpolate2(e,b)
            kerAcm = [kerAcm[jj]+kerInc[jj] for jj in range(numBins)]
        kerAcm = [kerAcm[jj] / float(samples) for jj in range(numBins)]
        ker.append (kerAcm)
    self.redKer = numpy.asarray(ker).transpose()
    return
```

The 61 by 61 DRF matrix for PVT is illustrated in Figure 13. The height of the matrix element indicates the number of counts in a detection channel per incident gamma in an incident channel.

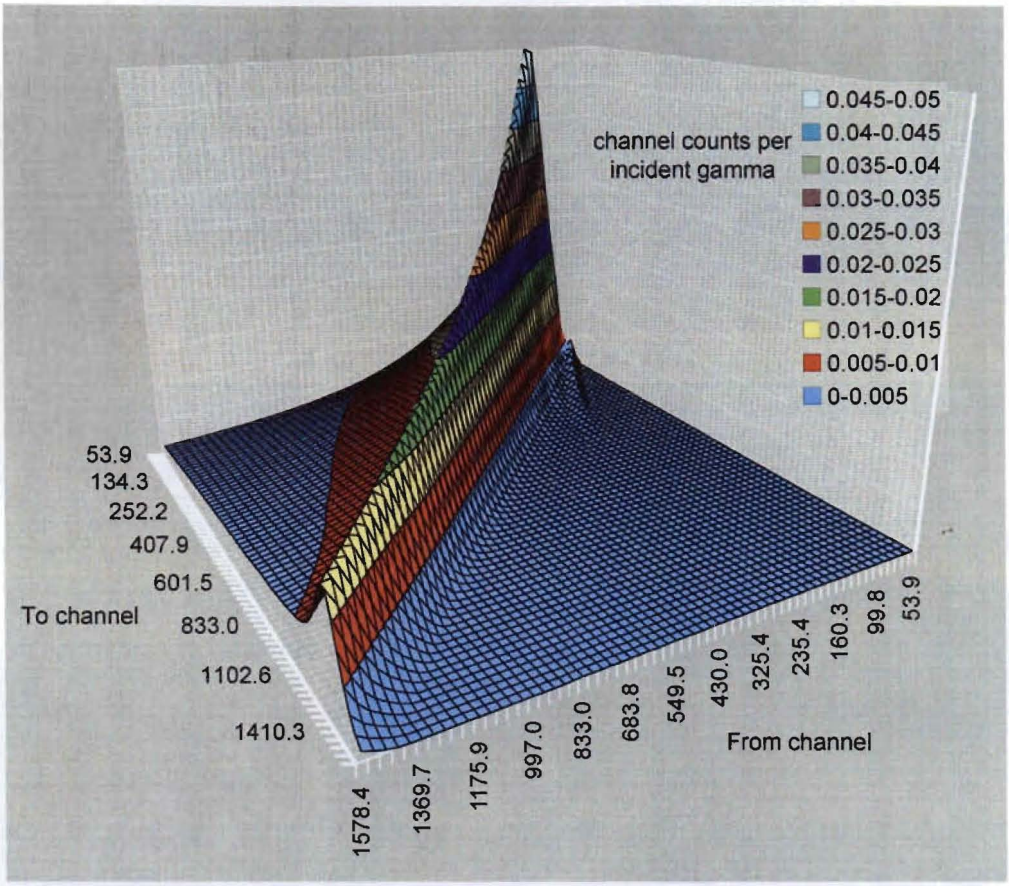

Figure 13. Three dimensional representation of the 61 x 61 DRF matrix for 5 cm thick PVT detector material, constructed with the algorithm described in the text from twelve detailed MCNPX runs.

7 Example Application of Algorithm

The nominal unshielded HEU source produces a flux of 25,092 gammas per (m^2 s) in the 50 to 1001 keV range, at a distance of 5 meters. For a PVT detector with minimum detection energy of 50 keV and maximum detection energy of 1600 keV, the NDFOM methodology uses 61 non-uniform channels. The incident HEU flux by channel is shown in Figure 14. The matrix product of the 61 by 61 DRF matrix with the vector of incident channel fluxes produces the vector of channel counts per (m^2 s), which is also shown in Figure 14.

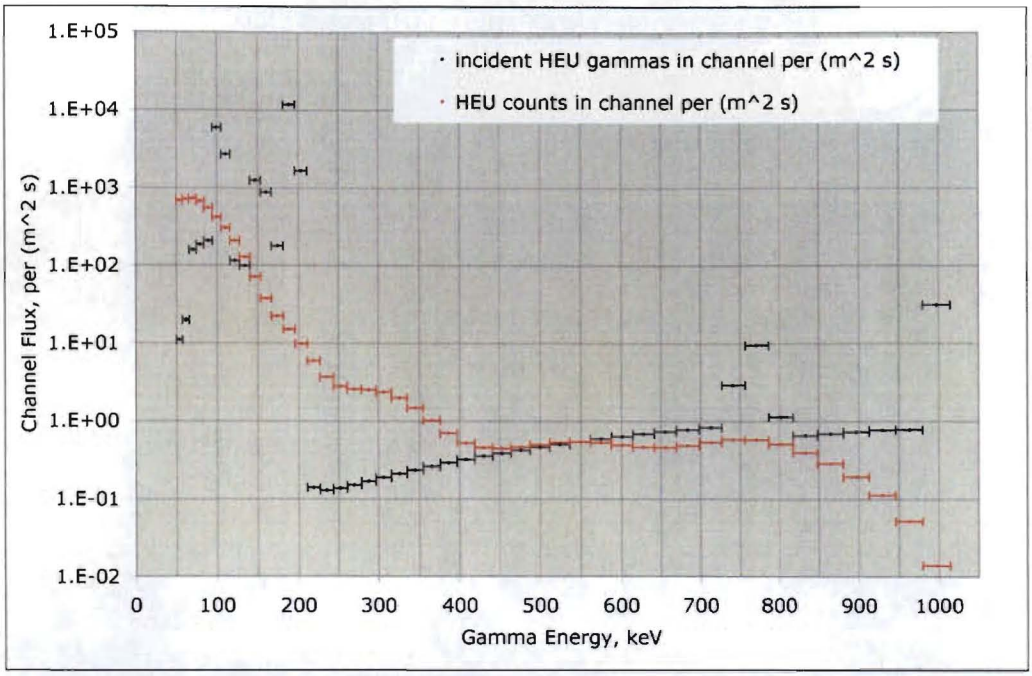

Figure 14. Incident flux by channel, 5 m from an HEU source, and the detected flux, accounting for the PVT detector response function.

The flux by channel is converted to counts by channel by multiplying the fluxes by the detector area and the scan time. For a large-panel PVT detector with 1 m^2 area, with a 1 second scan time, there would be 4642 counts from an HEU source 5 meters from the detector, and 7568 counts due to the background, counting all detection energies from 50 to 1600 keV. The total count signal-to-noise ratio would thus be 53.4. Using equation 2, a matched filter giving optimal weight to each channel would give an effective signal-to-noise ratio of 70.1.

8 Neutron Detector Efficiencies by Neutron Energy and Moderator Thickness

The neutron detection efficiency of a ^3He proportional counter, as detected counts per incident neutron, is much higher for thermal neutrons than for fast or epithermal neutrons. Mares[19] reports the detection efficiency of a ^3He proportional counter surrounded by 13 different thicknesses of polyethylene moderator (ranging from 0 to 15 inches), for 27 different neutron energies (ranging from 0.01 eV to 30 MeV). The detector was a 3.2 cm diameter sphere, and thus had a cross-sectional area of 8.04 cm^2, and an average thickness of 2.13 cm. It had a ^3He fill pressure of 1.75 atmospheres. To get the detector efficiency for the three neutron groups used in NDFOM, we average the detector efficiency over the

[19] Vladimir Mares, Gertrude Schraube and Hans Schraube, *Calculated neutron response of a Bonner sphere spectrometer with ^3He counter*, Nuclear Instruments and Methods in Physics Research A, Vol. 307, North Holland, pp. 398-412, 1991.

energy spectra of each of the three groups: a Maxwellian thermal spectra at T=320 °K, a 1/E epithermal spectrum from 0.5 eV to 100 keV, and a Maxwellian fission neutron spectrum at T=1320 keV. The detection efficiencies from the Mares data for each of the three groups is shown as a function of moderator thickness in Figure 15. As moderator thickness increases, the detection efficiency of thermal neutrons drops due to increasing neutron absorption. For epithermal and fast neutrons, the detection efficiency first increases as more neutrons get moderated to thermal energies, and then decreases as absorption begins to become important. In NDFOM, the analyst enters the moderator thickness as a parameter of the detector. For epithermal neutrons, the peak detection efficiency occurs for a moderator thickness of 8.5 cm, and for fast neutrons, the peak occurs at a moderator thickness of 16 cm.

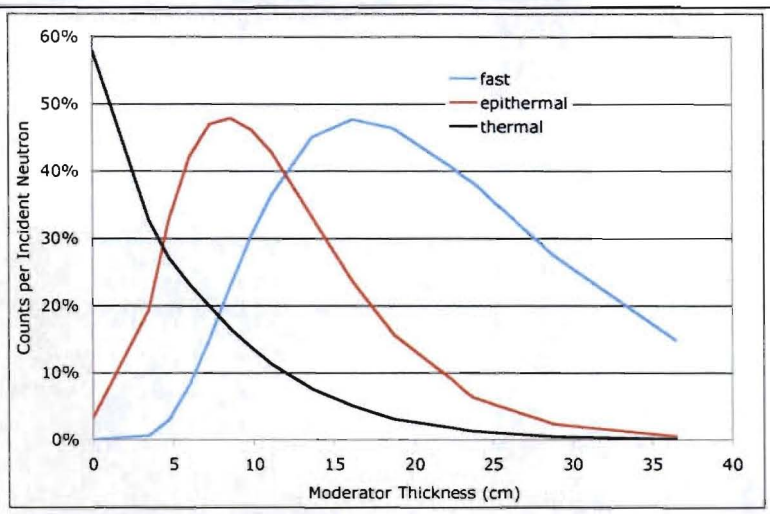

Figure 15. Neutron detection efficiency for a 5 cm diameter He-3 tube (average thickness = 3.93 cm) for thermal, epithermal, and fast neutrons, for various polyethylene thicknesses, from [Mares].

A validation benchmark is based on another experimental measurement series[20], which evaluated the detection efficiency of a SAM935 detector with the optional neutron detector installed. This moderated ^{3}He detector is 1.14 cm diameter and 10.2 cm long. They report a measured absolute detection efficiency of 4.6 10-6 at a distance of 1 meter, with 9 cm of moderator internal to the sensor, and no additional moderator, which equates to an intrinsic detection efficiency of 5.0%, for a fast neutron spectrum generated by a ^{252}Cf source. The NDFOM algorithm described above computes an intrinsic efficiency of 5.8% for a fast neutron spectrum for a moderator thickness of 9 cm. The LANL experiment also reported an absolute detection efficiency of $1.4x10^{-5}$ at a distance of 1 meter when a 6.35 cm polyethylene moderator is placed between the source and the detector, which equates to an intrinsic efficiency of 15.2%. The NDFOM neutron detection algorithm computes an intrinsic efficiency of 13.7% for a total moderator thickness of 16 cm.

[20] Mark A. Nelson, David Daily, and Mohini Rawool-Sulivan, *Evaluation of Neutron-Capable Handheld Devices*, Los Alamos National Laboratory report LA-UR-04-1694.

9 Concluding Remarks

NDFOM uses a first-principles approach for computing the ability of radiation detectors to detect radiating materials of interest. The approach is anchored on high fidelity simulations with the Monte Carlo particle and radiation transport code MCNP-X, augmented by link analyses, spectra transformation algorithms, interpolation algorithms and radiation attenuation and build-up analyses. The physics and mathematics modeling approach provides a context for understanding tests and evaluations of equipment conducted with materials of interest.

Radiation spectra have been constructed for significant quantities of special nuclear materials, in particular the fissile isotopes uranium-235 and plutonium-239. We also describe the construction of spectra for other radiating materials of interest, including gamma emitters ^{137}Cs, ^{60}Co and ^{192}Ir, the beta-bremsstrahlung emitter ^{90}Sr, and neutron sources ^{238}Pu, ^{252}Cf and ^{241}AmBe.

In order to implement an analysis tool that an analyst can use to rapidly evaluate the performance of detectors, we have found several useful algorithmic approaches. The underlying principle is to make use of a limited number of pre-run high-fidelity MCNPX simulations to generate spectra and detector response function benchmarks, and then build the code needed to interpolate and extrapolate from these benchmarks to the scenarios of interest. Computation efficiency was significantly increased without sacrificing fidelity by using a variable-width energy bin structure to represent the detector response functions.